Available online at www.sciencedirect.com

ScienceDirect

Procedia Engineering 207 (2017) 2161–2166

Procedia Engineering

www.elsevier.com/locate/procedia

International Conference on the Technology of Plasticity, ICTP 2017, 17-22 September 2017, Cambridge, United Kingdom

Anisotropy influence on flow behaviour and plastic instability of Ti6Al4V sheets deformed in a wide range of temperatures and strain rates

Q.L. Wang[a], M.F. Novella[a], A. Ghiotti[a], S. Bruschi[a]*

[a]*Department of Industrial Engineering, University of Padova, Via Venezia 1, 35131, Padova, Italy*

Abstract

Ti6Al4V sheets are usually difficult to form at room temperature as a consequence of their reduced number of slip systems. The heating of the alloy below the β-transus temperature is recognized to enhance its formability, reducing the flow stress and increasing the ductility. However, the effect of the sheet anisotropy on the material flow behaviour and plastic instability at varying temperature and strain rate has not been studied systematically, yet. To this aim, uniaxial tensile tests were carried out in a wide range of testing temperatures (from room temperature to 800°C) and strain rates (0.01, 0.1, 1 s^{-1}) to assess the anisotropy effects. Strain hardening, strain rate sensitivity, and Lankford coefficients were evaluated as a function of the testing parameters and sample orientation. Furthermore, a numerical model of the uniaxial tensile tests was developed and calibrated making use of the Barlat-Lian-1989 yield criterion and a hardening rule, which was adapted to take into account the anisotropic behaviour at different temperatures. It was proved that the developed model was capable of predicting the strain localization in the sample gauge length due to plastic instability as well as its thickness distribution at varying temperature and strain rate.

Keywords: Ti6Al4V; anisotropy; sheet forming; high temperature; flow behaviour; plastic instability.

1. Introduction

Titanium alloy Ti6Al4V sheets are of interest of aerospace, biomedical and chemical fields, thanks to their attractive properties such as good biocompatibility, high strength-to-weight ratio, and elevated corrosion resistance [1]. However, as a consequence of the reduced number of slip systems, they are characterized by poor formability at

* Corresponding author. Tel.: +39 049 8276821; fax: +39 049 8276816.
E-mail address: stefania.bruschi@unipd.it

1877-7058
10.1016/j.proeng.2017.10.975

room temperature, making usually necessary high temperature processing in order to be properly formed. Moreover, the Ti6Al4V dominating Hexagonal Close-Packed (HCP) structure may induce significant anisotropy of the mechanical characteristics [2], which can be of great concern in sheet metal forming, since the as-delivered sheet texture may enhance the material anisotropic characteristics.

The literature review presents a few papers devoted to the experimental evaluation of the anisotropic characteristics of titanium alloys sheets, most of which refer to room temperature testing as in [3] in case of commercially pure titanium thin sheets and in [2] for α-titanium. In [4] the anisotropy of a near α-titanium alloy was evaluated at 600°C, but focusing on the alloy service life characteristics. In [5] the mechanical behavior of Ti6Al4V sheets was modelled using different anisotropic yield criteria that were calibrated through tensile and compression tests for different sample orientations, but the investigation was restricted to room temperature. On the contrary, th modelling of the Ti6Al4V behaviour at elevated temperature was reported for low strain rate values, typical of superplastic forming, but neglecting any influence of the material anisotropy [6-7].

To this regard, the research work here presented has a twofold objective: (i) to investigate the anisotropy effects on the Ti6Al4V flow behaviour and plastic instability in a wide range of thermo-mechanical conditions, typical of industrial sheet forming operations, and (ii) to assess the capability of a properly calibrated numerical model of the tensile test to adequately predict the plastic instability in terms of strain field and sample thickness evolution regardless of the testing temperature. To achieve the former target, the anisotropy influence on the plastic behavior of the material was investigated by means of tensile tests carried out in a wide range of temperatures and strain rates. The latter target, on the other hand, was pursued by implementing into the tensile test numerical model the Barlat-Lian-1989 yield criterion [8] calibrated through the experimental outcomes and adapted to take into account the Ti6Al4V anisotropic behaviour at different temperatures.

2. Experiments

2.1. Experimental apparatus and procedure

The tensile test samples were laser-cut along three directions (namely 0°, 45° and 90° with respect to the rolling direction) from 1 mm thick-sheets of Ti6Al4V, provided in the annealed condition characterized by an equiaxed α + β microstructure. The tensile tests were carried out on a 50 kN universal MTSTM hydraulic testing machine. The testing temperatures were in the range from room temperature to 800°C, while the nominal strain rates were set at 0.01, 0.1 and 1 s^{-1}, as reported in the experimental plan of Table 1. To heat the samples up to the testing conditions, the temperature was measured by a k-type thermocouple spot-welded on the sample central zone and the signal was used as a feedback for the closed-loop control system driving the induction heating system integrated in the experimental apparatus. The sample temperature field was also monitored through an infrared thermocamera to calibrate afterwards the numerical model. After a soaking time of 30 s, the samples were strained until fracture at constant strain rate. During testing, the sample deformation was recorded through a CCD camera, and its acquisitions were used in the Aramis^{TM} system to calculate the evolution of the true strain.

Table 1. Experimental plan.

Temperature (°C)						Strain (-)	Strain rate (s^{-1})	Orientation (-)
25	200	400	600	700	800	ε	0.01	0°, 45°, 90°
25	200	400	600	700	800	ε	0.1	0°, 45°, 90°
25	200	400	600	700	800	ε	1	0°, 45°, 90°

2.2. Flow behaviour and plastic anisotropy

Ti6Al4V exhibited a non-identical response in terms of flow behaviour and strain at fracture for different sample orientations. Fig. 1 (a) shows the influence of the temperature and sample orientation on the Ultimate Tensile Strength (UTS) values for a strain rate equal to 0.1 s^{-1}: as expected, UTS decreased at increasing temperature regardless the sample orientation. On the other hand, samples oriented at 45° with respect to the rolling direction showed the lowest strength regardless the testing temperature, whereas samples oriented at 0° and 90° were characterized by comparable UTS values.

The influence of the temperature and sample orientation on the strain hardening exponent is shown in Fig. 1 (b) for the same strain rate. As expected, the strain hardening decreases at elevated temperatures, reaching values close to zero at the highest one. Again, a strong influence of the sample orientation was evident.

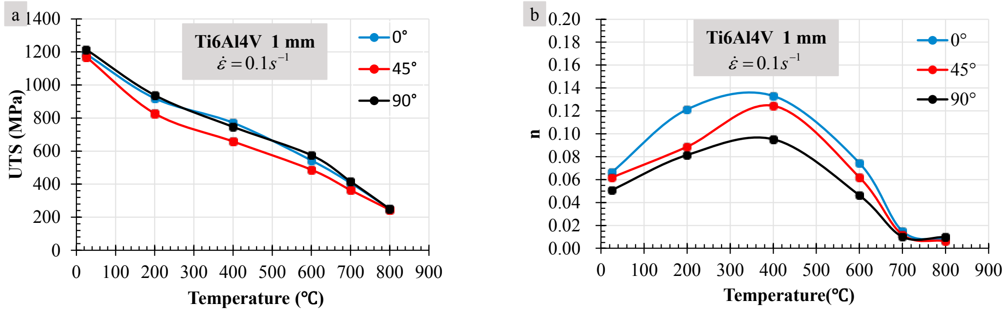

Fig. 1. (a) UTS and (b) strain hardening exponent as a function of the testing temperature and sample orientation(± 2% uncertainty).

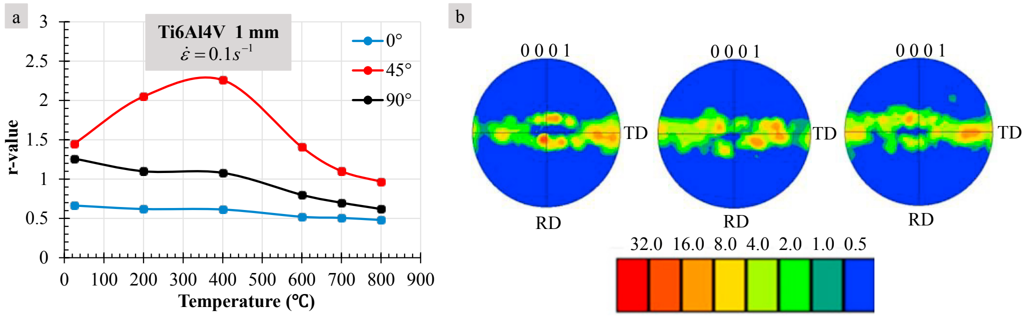

Fig. 2. (a) Plastic normal anisotropy as a function of the testing temperature and sample orientation(± 2% uncertainty), and (b) pole figures at room temperature, 600°C and 800°C for the sample oriented at 0°.

The plastic normal anisotropy, expressed as the Lankford or anisotropy coefficient *r* that is the ratio between the sample strain in the width and the one in the thickness as recorded by the Aramis^{TM} system, is shown in Fig. 2 (a) as a function of the testing temperature and sample orientation. The effect of temperature is noticeable: a decrease of the *r* values is evident for the samples oriented at 0° and 90° at increasing temperature. The 0° oriented samples have always values lower than 1, whereas the 90° oriented samples tend to be isotropic in the temperature range between room temperature and 400°C. On the other hand, the trend of the 45° oriented samples is pretty different, with an initial increase of the plastic anisotropy in the low temperature range and subsequent decrease at higher temperatures.

To account for this still anisotropic behaviour at elevated temperature, Electron Back Scattered Diffraction (EBSD) analysis was carried out for the samples oriented at 0° and strained at room temperature, 600°C, and 800°C. After standard metallographic preparation, the samples were finished with a vibratory polishing using an acid solution containing 0.02 μm colloidal silica. Fig. 2 (b) shows the texture plots for the RD-TD plane. It is evident a strong $(0001)_\alpha$ accumulation along the axis in the TD direction and weak $(0001)_\alpha$ accumulation along the axis in the RD direction, indicating strong T-texture and weak basal-texture (B texture) components, more pronounced at room temperature, but still present at elevated temperature.

The aforementioned behaviour was observed for all the other tested strain rates.

2.3. Plastic instability

The strain rate sensitivity exponent *m*, indicative of the occurrence of either localized or diffuse necking, was calculated using an exponential law to model the flow stress as a function of the strain rate. Fig. 3 (a) shows the *m* values as a function of the temperature and sample orientation at a strain rate equal to 0.1 s^{-1}. The material always exhibited positive *m* values for all the testing temperatures. Nevertheless, in the range of temperatures between 0° and 400°C, the values were close to zero regardless of the sample orientation, meaning that the plastic instability manifested itself as localized necking. Starting from 600°C, the strain rate sensitivity became higher, with an increase at increasing temperature. Furthermore, it can be noted that the *m* values for the samples oriented at 45° were always higher than the ones of the samples oriented at 0° and 90°. The drastic increase of the strain rate sensitivity in the range of elevated temperatures was indicative of the occurrence of plastic instability in form of diffuse necking, as witnessed in Fig. 3 (b) by the Aramis™ images of the samples strained till fracture. Samples oriented at 45° showed a larger diffuse necking in the temperature range between 600° and 800°C, consistent with their higher ductility at increasing temperature, compared to the samples oriented at 0° and 90°. It is worth to note that at 600°C, the 90° sample showed the lowest *m* value, and from the Aramis™ images the necking was still localized. Same results were obtained for the other tested strain rates.

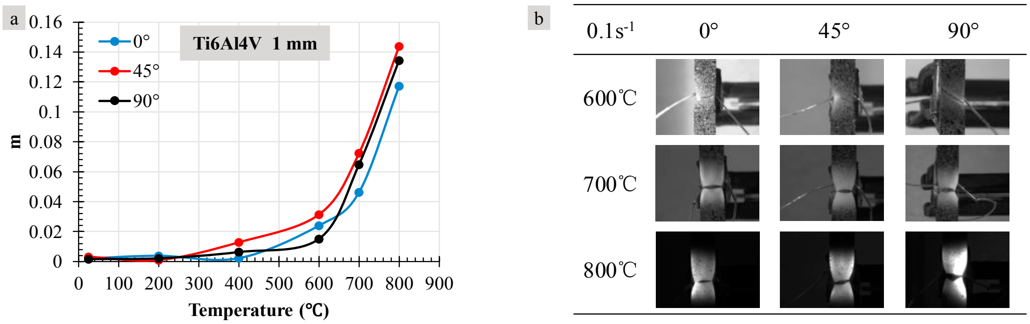

Fig. 3. (a) Strain rate sensitivity as a function of the testing temperature and sample orientation; (b) Aramis™ images of the samples strained at elevated temperatures and strain rate of 0.1 s^{-1}.

Numerical model

The numerical model of the tensile tests was developed with the LS-Dyna™ code, using a dynamic-implicit analysis and a coupled thermo-mechanical solution procedure. Due to the high length-to-thickness and width-to-thickness ratios that characterize the sample geometry, shell quadrangular elements were used following the fully integrated Hughes-Liu formulation with 7 through-thickness integration points. The sample heating to the testing temperature was simulated implementing a localized heat generation source to the sample central zone, with the same dimensions of the inductor head. A thermal soaking time of the same duration of the experimental one was simulated in order to reach steady-state temperature distribution along the sample axis.

The Ti6Al4V behavior was modelled with the following characteristics:

- Temperature-dependent values of the Young's and Poisson's moduli from literature [9];
- Temperature and strain rate-dependent anisotropic yield locus on the basis of the Barlat-Lian-1989 yield criterion, implemented by using the Lankford coefficients at varying temperature and strain rate;
- Crystallographic constant *m* of the Barlat-Lian-1989 yield criterion set equal to 12, which is stated in literature [5] to be the most accurate value for HCP crystal lattice at room temperature. Being all the tests carried out below β-transus temperature in a range of temperatures where there is still little β-transformation, the HCP crystal lattice can be assumed to be the dominating structure for all the testing conditions;
- Temperature and strain rate-dependent hardening rule, implemented by using the experimental flow curves derived from samples oriented at 0°;
- Orientation-dependent strain rate sensitivity, implemented changing the hardening rule as a function of the specimen orientation; this feature is essential to capture the behavior highlighted in Fig. 3.

The experimental and numerical results were compared in order to assess the capability of the model to predict the plastic straining regime of the sample. In particular, the major strain and thickness distribution along the sample axis were assessed, making use of the Aramis™ data, consisting of local strain measurements during the whole test duration. The baseline strain rate of 0.1 s^{-1} was used for the comparison and two temperatures were chosen for the validation, namely 200°C and 700°C, representative of the occurrence of two distinct plastic instability phenomena, localized necking for the former and diffuse necking for the latter. Furthermore, the choice of these two temperatures allowed evaluating the model predictability in cold conditions, where the material strain hardening was predominant, as well as in hot conditions, where the strain rate sensitivity played the major role. In all the conditions the benchmark was carried out after the plastic instability onset, at approximately the same amount of equivalent strain, namely 0.2.

Fig. 4 illustrates the comparison at 200°C. For the 0° and 45° directions, the model was capable of predicting both the major strain field and thickness distribution along the sample axis. In particular, the thickness distribution prediction was accurate both in the necking zone and outside it, proving that the temperature softening and the strain hardening parameters of the model were properly set. For the 90° direction, the major strain distribution shape was less accurate, although the maximum value was correct as well as the thickness distribution.

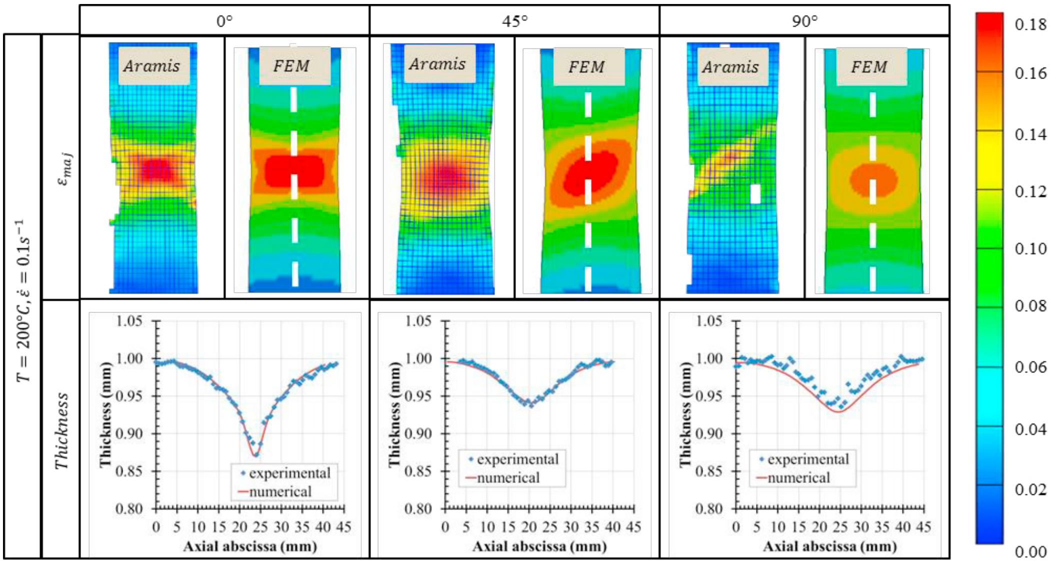

Fig. 4. Experimental and numerical benchmark at 200°C, strain rate 0.1 s^{-1}.

Fig. 5 shows the same results for 700°C. The prediction accuracy was also high, particularly the strain distribution along the axis, which showed the typical characteristics of the hot deformation regimes, namely an almost negligible uniform deformation (blue zones at the sample extremities in both experimental and numerical fringe maps) and a larger post-necking strain diffusion.

A validation case is shown in Fig. 6, where the comparison between the experimental and numerical thickness distributions at varying rolling direction at 650℃ and strain rate of 0.1 s^{-1} (testing conditions not used for the model calibration) further proved the accuracy of the developed numerical model.

Conclusions

On the basis of the outcomes from uniaxial tensile tests, the paper showed that the anisotropic characteristics of Ti6Al4V sheets influenced the material behaviour in a wide range of temperatures from room temperature to 800°C. It can be concluded that anisotropy and temperature had a strong influence on the strain hardening exponent and strain rate sensitivity, especially at the 45° direction, but UTS decreased at increasing temperature regardless of the sample orientation. It can be noted that anisotropic behaviour was pronounced at room temperature, but still present at elevated temperature, the texture evidenced by EBSD measurements.

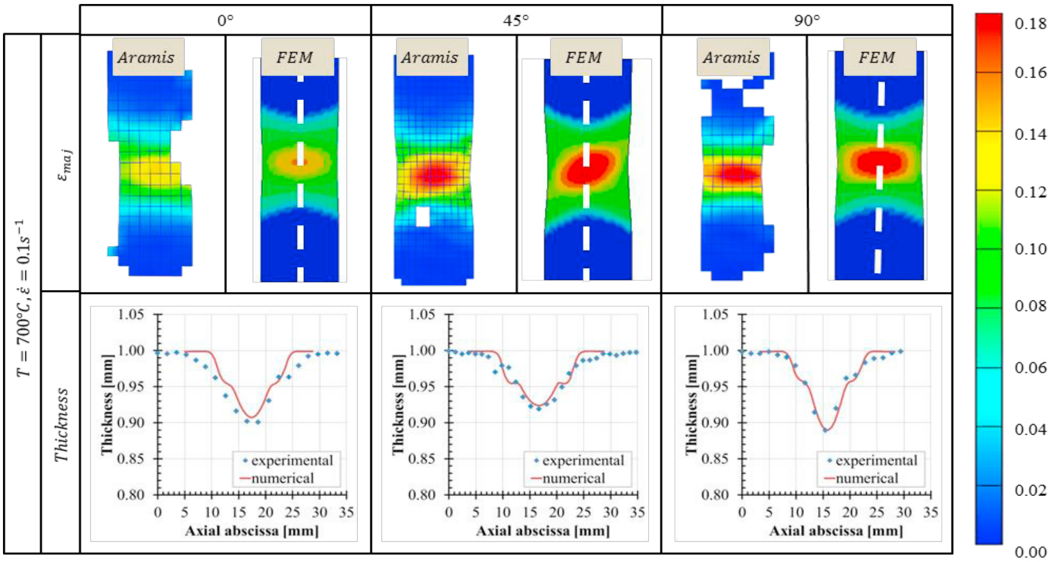

Fig. 5. Experimental and numerical benchmark at 700°C, strain rate 0.1 s^{-1}.

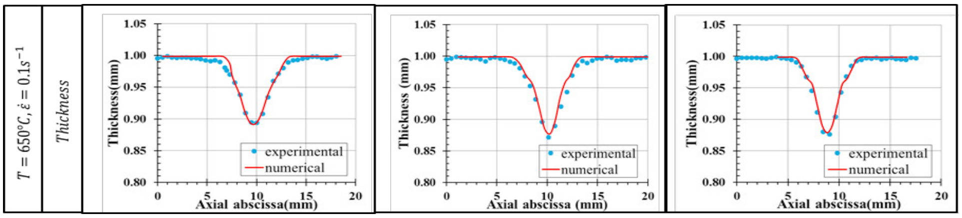

Fig. 6. Experimental and numerical benchmark at 650°C, strain rate 0.1 s^{-1} (validation case).

The use of the Barlat-Lian 1989 yield criterion and the adaption of the hardening rule to account for the anisotropic behaviour at different temperatures made possible to validate the developed numerical model of the tensile tests assessing the agreement between experimental and numerical results in terms of strain field and thickness distribution after plastic instability. High accuracy and reliability in predicting the experimental results were shown.

Acknowledgements

The financial support of the China Scholarship Council (CSC) (No. 201608370094) is gratefully acknowledged.

References

[1] C. Leyens, M. Peters, Titanium and Titanium Alloys, John Wiley & Sons, Weinheim, 2003.
[2] A. Roth, M.A. Lebyodkin, T.A. Lebedkina, Mechanisms of anisotropy of mechanical properties of α-titanium in tension conditions, Mat. Sci. Eng. A. 596 (2014) 236-243.
[3] H. Nasiri-Abarbekoh, A. Ekrami, A.A. Ziaei-Moayyed, Effects of thickness and texture on mechanical properties anisotropy of commercially pure titanium thin sheets, Mater. Des. 44 (2013) 528-534.
[4] W.Y. Li, Z.Y. Chen, J.R. Liu, Effect of texture on anisotropy at 600℃ in a near-α titanium alloy Ti60 plate, Mat. Sci. Eng. A. 688 (2017) 322-329.
[5] O.M. Badr, F. Barlat, B. Rolfe, Constitutive modelling of high strength titanium alloy Ti-6Al-4V for sheet forming applications at room temperature, Int. J. Solids. Struct. 80 (2016) 334-347.
[6] N. Kotkunde, A.D. Deole, A.K. Gupta, Comparative study of constitutive modeling for Ti-6Al-4V alloy at low strain rates and elevated temperatures, Mater. Des. 55 (2014) 999-1005.
[7] J. Xiao, D.S. Li, X.Q. Li, Constitutive modeling and microstructure change of Ti-6Al-4V during the hot tensile deformation, J. Alloys Compd. 541 (2012) 346-352.
[8] F. Barlat, J. Lian, Plastic behaviour and stretchability of sheet metal, Part I: A Yield function for orthotropic sheets under plane stress conditions, Int. J. Plasticity 5 (1989) 51-66.
[9] R. Boyer, E.W. Collings, G. Welsch, Materials Properties Handbook: Titanium Alloys, ASM International (1994).